ORIGINAL ARTICLE

Localized RNA interference therapy to eliminate residual lung cancer after incomplete microwave ablation

Fei Cao[1]*, Chao Wan[2]*, Lin Xie[1]*, Han Qi[1]*, Lujun Shen[1], Shuanggang Chen[1], Ze Song[3] & Weijun Fan[1]

1 Department of Minimally Invasive Interventional Center, Sun Yat-sen University Cancer Center, State Key Laboratory of Oncology in South China, Collaborative Innovation Center for Cancer Medicine, Guangzhou, China
2 Department of Oncology, Shandong Provincial Hospital Affiliated to Shandong University, Jinan, China
3 Department of Oncology, The Seventh Affiliated Hospital, Sun Yat-sen University, Shenzhen, China

Correspondence
Weijun Fan, Department of Minimally Invasive Interventional Center, Sun Yat-sen University Cancer Center, State Key Laboratory of Oncology in South China, Collaborative Innovation Center for Cancer Medicine, No. 651 Dongfeng Road East, Guangzhou, Guangdong 510060, China.
Tel: +86 20 8734 3271
Fax: +86 20 8734 3271
Email: fanweijun1964@126.com

*These authors contributed equally to this work.

Abstract

Background: This study evaluated the safety and efficacy of localized injection of polyethylene glycol (PEG)-hyperbranched polyethyleneimine (PEI)-EGFR-small interfering RNA (siRNA) nanocomposites as a treatment for residual lung cancer after incomplete microwave ablation (MWA).

Methods: Human lung cancer cell lines with high and low EGFR expression were selected for the study. The effects of PEG-PEI-EGFR-siRNA nanocomposite transfection on the proliferation, migration, and apoptosis of lung cancer cells were verified. Sixteen healthy ICR mice were injected into the lung to test the biological safety of the nanocomposites. In addition, 24 subcutaneous xenograft BALB/C nude mice with high EGFR expression were separated into four groups and then treated with an intratumoral injection of PEG-PEI-EGFR-siRNA, PEG-PEI-normal control (NC)-siRNA, PEG-PEI-EGFR-siRNA after MWA, or PEG-PEI-NC-siRNA after MWA. Tumor growth, pathological changes, and EGFR expression in each group were observed.

Results: PEG-PEI-EGFR-siRNA nanocomposites were transfected to HCC 827 cells showing high EGFR expression and to H23 cells showing low EGFR expression. In HCC827 cells, downregulation of EGFR gene expression reduced cell proliferation, invasion, and migration, whereas cell apoptosis increased. In contrast, in H23 cells, no significant differences in those parameters were detected. No acute toxicity occurred in the ICR mice during the biosafety test. Localized injection of PEG-PEI-EGFR-siRNA nanocomposites significantly inhibited the growth of human lung xenografts in mice and the growth of residual tumors after MWA.

Conclusion: PEG-PEI-EGFR-siRNA nanocomposites may be a supplemental therapy strategy to treat residual lung cancer after incomplete MWA.

Introduction

Primary lung cancer is a leading cause of cancer-related death worldwide. Every year, 1.8 million people are diagnosed with lung cancer and 1.6 million people die from this disease.[1,2] Surgery is the recommended treatment for early stage non-small cell lung cancer (NSCLC). For patients who are not appropriate candidates or who refuse surgery, stereotactic body radiotherapy (SBRT) and computed tomography (CT)-guided ablation techniques are appropriate alternatives.[2,3] CT-guided ablation can locally heat tumors to induce coagulation necrosis while causing minimal damage to normal lung tissue. Many studies have proven that it is a safe and effective treatment option for lung cancer patients.[4–6] However, high residual and tumor recurrence rates after ablation remain. A prospective study reported a local recurrence rate of 40% two years after radiofrequency ablation, significantly lower than the rates after SBRT or sublobar resection.[7–9]

In advanced and metastatic NSCLC, the most frequent applicable alteration is *EGFR* mutation. The approval of EGFR-tyrosine kinase inhibitors (TKI) has pushed the

development of target therapy;[10] however, after EGFR-TKI treatment, almost all patients eventually show disease progression as a result of acquired resistance.[11] The RNA interference (RNAi) technique, a biological process to suppress genetic expression, was first developed in 1998.[12] Since RNAi was developed 20 years ago, scientists have continued attempting to apply this technology in new treatments for various diseases. In 2018, the US Food and Drug Administration approved the world's first RNAi drug, patisiran, which specifically inhibits hepatic synthesis of transthyretin. The APOLLO phase 3 trial proved that patisiran was beneficial to patients with hereditary transthyretin amyloidosis. The approval of patisiran may finally lead to the development of RNAi drugs.[13–15] Nanoparticle-mediated siRNA treatment is expected to be an alternative to chemotherapy for lung cancers. Many kinds of small interfering RNA (siRNA) therapy have been promoted, including VEGF, EPHA2, and PKN3. However, challenges regarding the delivery, safety, and stability of siRNA remain.[16] To date, no single siRNA therapy has been used in a clinical setting for lung cancer. The clinical advancement of siRNA treatment depends on the development of safe and effective gene delivery systems, including lipid and polymer-based systems and rigid nanoparticles. Among these systems, polyethyleneimine (PEI) derivative systems have promising practical application in the future, and are used as the gold standard in siRNA delivery applications.[17] Many studies have found that radiofrequency ablation could also lead to significant increases in the delivery of drug-loaded nanoparticles around ablation zones and improve the focal delivery of siRNA to target tissues.[18,19] In this study, a new polyethylene glycol (PEG)-hyperbranched-PEI-EGFR-siRNA nanocomposite was used to eliminate residual lung cancer after microwave ablation (MWA) in an attempt to solve the problems of high residual and recurrence rates after local ablation of lung cancer.

Methods

Cell lines

All lung cancer cell lines used in this study were obtained from the molecular imaging laboratory at the Sun Yat-sen University Cancer Center. The HCC827, H23, and H2228 lung cancer cell lines were cultured in RPMI-1640 medium, whereas the PC9 cancer cell line was cultured in Dulbecco's modified Eagle medium supplemented with 10% fetal bovine serum (Gibco, Grand Island, NY, USA). EGFR expression in different cell lines was compared using Western blot.

Nanoparticle small interfering RNA (siRNA) formulation

As a first step, the terminal hydroxyl group of PEG was activated by carbonyl diimidazole (CDI), and the activated PEG was reacted with PEI to form PEG-PEI. The polymer was then dissolved in phosphate buffer solution (pH 7.4) to a concentration of 1 mg/mL, whereas siRNA was dissolved in deionized water to a concentration of 0.5 μg/μL. Finally, the two solutions were mixed together in an N/P ratio of 6 (ratio of amino groups in a polymer to phosphate groups in a nucleic acid), and the mixture was shaken vigorously for 30 seconds. The mixture was then allowed to stand for 30 minutes to obtain a nanocomposite solution.

In vitro transfection

Human lung cancer cell lines with high and low EGFR expression were seeded on six-well plates, supplemented with 2 mL of RPMI-1640 medium containing fetal bovine serum and antibiotics, and incubated at 37°C with 5% CO_2 in a humidified incubator until reaching 50–60% confluence within 24 hours. The cells were allocated into three groups: mock (0.5 ml of transfection reagent), EGFR-siRNA (0.5 ml of EGFR-siRNA nanocomposite), and normal control (NC)-siRNA (0.5 ml of NC-siRNA nanocomposite) groups. The siRNA of the EGFR sequence was 5′-CCUAUGCCUUAGCAGUCUUTT-3′, 5′-AAGACUGCUAAGGCAUAGGTT-3′. The effects of the PEI-siRNA complex on cell proliferation, migration, and apoptosis were evaluated. A Cell Counting Kit 8 (CCK-8) was used to determine cell proliferation, 4′,6-diamidino-2-phenylindole (DAPI) staining was used to examine cell apoptosis, and the invasive ability was assayed using the transwell chamber method. All techniques were performed according to the manufacturer's instructions.

In vivo biological safety

All animal studies were performed with the approval of the Sun Yat-sen University Cancer Center. The biosafety test of PEI-siRNA complex was performed by intrapulmonary injection in 16 ICR mice (8 male, 8 female). Because mice have three right lungs but only one left lung, the left lung was selected for injection. The needle was inserted no more than 0.4 cm in depth. The experimental group was injected with 0.1 ml of nanocomposite mixture, whereas the control group was injected with 0.1 ml of normal saline. After the injection, the animals were subsequently observed once a day for 14 days. The mice were weighed at the same time points on days 2, 4, 6, 8, 10, 12, and 14 after injection, and then

sacrificed on the 14th day. After sacrifice, the heart, lung, thymus, liver, spleen, and kidney were dissected and weighed to calculate organ coefficients (organ weight [mg]/mouse body weight [g]). Lung tissue was fixed in 10% neutral formalin fixative, embedded in paraffin, sectioned, stained with hematoxylin and eosin, and examined under a light microscope. Blood samples were collected via the eyeball, and whole blood cell count and blood biochemical indicators were analyzed.

In vivo transfection

HCC 827 lung cancer cells were inoculated subcutaneously into the bilateral groin of 24 BALB/C nude mice. After inoculation, body weight and maximum tumor diameter were measured on days 3, 6, 9, 12, 15, 18, and 21. Tumor volume was calculated and a tumor growth curve was plotted. The experiments were performed when the tumor had grown to a diameter of approximately 1.5 cm. The 24 mice were randomly divided into four groups. Group A: intratumoral injection of PEI-EGFR-siRNA; Group B: intratumoral injection of PEI-NC-siRNA (control); Group C: intratumoral injection of PEI-EGFR-siRNA after MWA; and Group D: intratumoral injection of PEI-NC-siRNA group after MWA (MWA control). After anesthesia, MWA was performed under real-time ultrasound guidance along the longest diameter of the tumor, with the parameters set to 10W/20s. Ultrasound angiography was performed immediately after MWA. Each mouse was intratumorally injected with 1.0 nmol siRNA.[20] To ensure that all nanocomposite fluids covered the entire tumor range, ultrasound was used to guide the injection in real-time.

Tumor harvest

The tumor volume was calculated in each group on days 7, 14, and 21 after treatment. After 21 days of observation, the mice were sacrificed and the tumor tissues were carefully removed. Changes in tumor volume, as well as final tumor weight and volume measured at different times were used as indicators of the efficacy of the nanocomposite. EGFR messenger RNA (mRNA) and protein expression was examined in each group by quantitative real-time PCR and Western blotting respectively.

Real-time PCR, Western blotting, and immunohistochemical staining

Total RNA samples were isolated and reverse transcribed into complementary DNA, and quantitative PCR was then performed according to the manufacturer's instructions. The data obtained from each sample were normalized

to the expression level of glyceraldehyde 3-phosphate dehydrogenase (GAPDH). The primers used were as follows: human EGFR: forward, 5′- TTTGTGTTCCCGG ACATAGT-3′, reverse, 5′-TTTGTGTTCCCGGACATAGT-3′; GAPDH: forward, 5′-GGGAAACTGTGGCGTGAT-3′, reverse, 5′-GAGTGGGTGTCGCTGTTGA-3′. All PCR was performed in triplicate and no-template groups were built. The 2-[(Ct of EGFR)—(Ct of GADPH)] method was used to calculate the relative expression of target genes. Western blotting and immunohistochemical staining were performed to detect EGFR, according to the manufacturer's instructions. Rabbit anti-EGFR (1:1000, Abcam, Cambridge, MA, USA) was the primary antibody used.

Statistical analysis

Statistical significance between two groups was determined by unpaired two-tailed Student's *t*-test, and between multiple groups using one-way analysis of variance. Differences were considered significant when $P < 0.05$.

Results

In vitro results

We screened the HCC827 lung cancer cells, which showed high EGFR expression, and the H23 lung cancer cells, which showed low EGFR expression (Fig 1a), and successfully synthesized PEG-PEI-EGFR-siRNA nanocomposites. Forty-eight hours after transfection, the visible cell colonies were dramatically reduced in the EGFR-siRNA group (Fig 1b). Using CCK-8 assay (Fig 1c), DAPI staining (Fig 1d), scratch assay (Fig 1e), transwell assay (Fig 1f), and detection of EGFR protein expression (Fig 1g) after interference, we obtained the following results. The HCC827 EGFR-siRNA group showed stronger inhibition of cell proliferation than the NC-siRNA group. Compared to the cells transfected with NC-siRNA, the HCC827 cells transfected by EGFR-siRNA showed increased apoptosis and decreased invasion and migration activity. EGFR-targeting siRNAs significantly inhibited the expression of EGFR protein in HCC827 cells; however, no significant differences in EGFR protein expression were observed in H23 cells (Fig 1c–g).

Biosafety test of intra-pulmonary injection of polyethylene glycol (PEG) polyethyleneimine (PEI)-EGFR-siRNA nanocomposites

The biological safety of the nanocomposite-loaded siRNA was verified to eliminate the toxic effect of PEG-PEI-siRNA injection on the results of the other experiments in
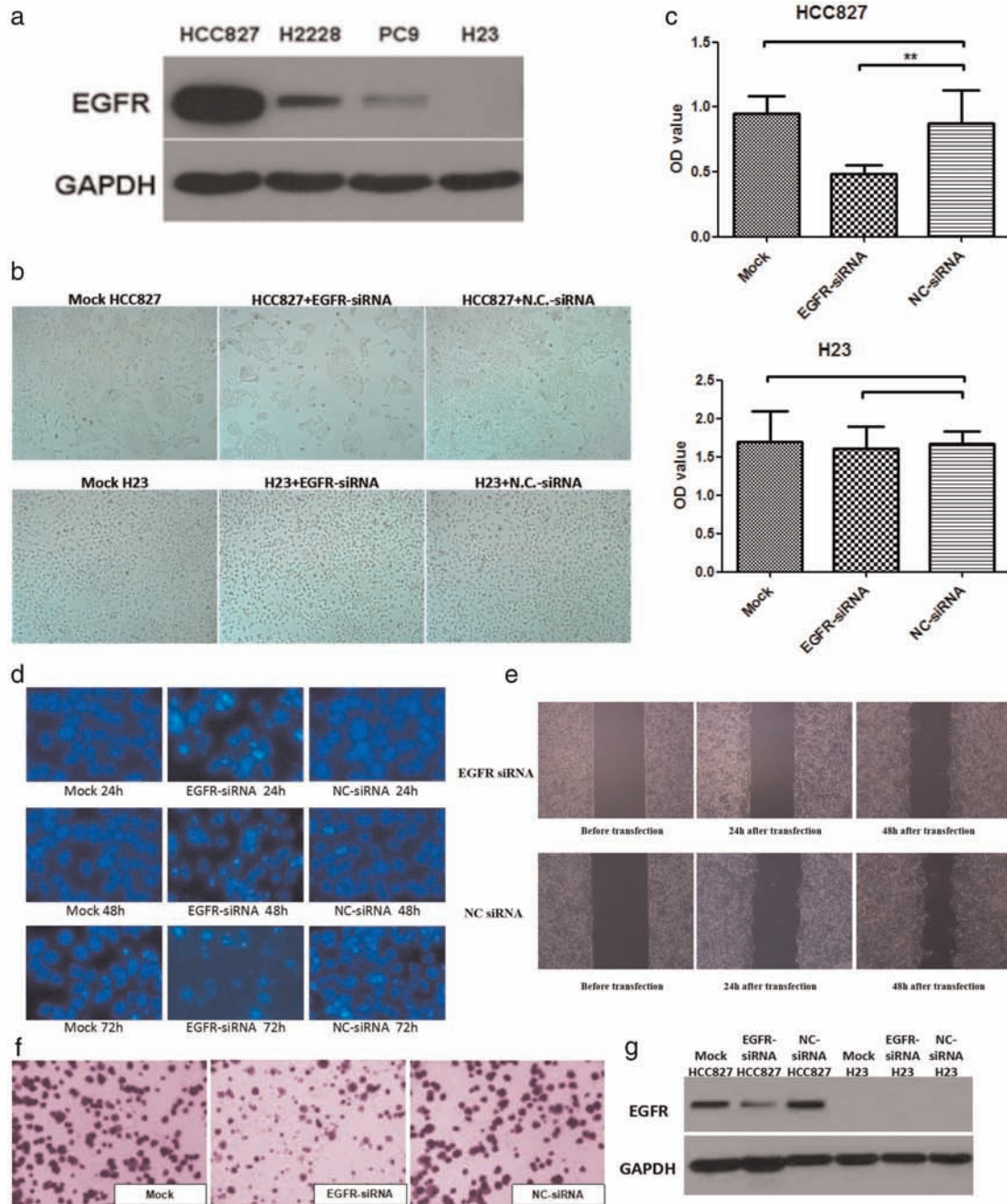
Figure 1 (**a**) EGFR protein expression in four non-small cell lung cancer (NSCLC) cell lines was detected by Western blotting. HCC827 cells with high EGFR expression and H23 cells with low EGFR expression were selected. (**b**) Microscopic observation of the growth of HCC827 and H23 cells at 48 hours after transfection with EGFR small interfering RNA (siRNA) and normal control (NC) siRNA. The number of cell colonies was reduced by EGFR-siRNA in HCC827 cells, but no significant difference was observed in H23 cells. (**c**) Cell Counting Kit 8 test results showed that after 72 hours of interference, the optical density (OD) values in HCC827 cells were significantly different after transfection with EGFR-siRNA and after transfection with NC-siRNA, whereas in H23 cells, there was no significant difference. (▧) Mock, (▨) EGFR-siRNA, and (▤) NC-siRNA. (**d**) Results of 4′,6-diamidino-2-phenylindole (DAPI) staining showed decreased apoptosis in the mock (transfection reagent only) and NC-siRNA groups, and increased apoptosis in the EGFR-siRNA group at 24–48 hours, with chromatin breakdown occurring at 72 hours. (**e**) Scratch test results showed that the EGFR-siRNA group had lower mobility between 12 and 24 hours after interference than that in the NC-siRNA group ($P < 0.001$). (**f**) Transwell assay results showed no significant difference in migration between the mock and NC-siRNA groups ($P = 0.063$), while knockdown of EGFR significant enhanced the migration ($P < 0.001$). (**g**) Western blotting results showed that EGFR-siRNA induced a significant decrease in EGFR protein expression in HCC827 cells. GAPDH, glyceraldehyde 3-phosphate dehydrogenase.

Table 1 Biosafe test: Biochemical and blood routine indicators of experimental and control mice

Indicator	Test	Control	*P* values
WBC 10E9/L	6.54 ± 1.32	8.10 ± 1.90	0.08
RBC 10E12/L	9.08 ± 0.55	8.97 ± 0.48	0.67
HGB g/L	144.50 ± 9.26	144.63 ± 5.93	0.98
PLT 10E9/L	850.75 ± 466.85	978.00 ± 408.22	0.75
HCT %	54.71 ± 2.80	55.00 ± 1.77	0.81
MCV fL	60.31 ± 2.19	61.20 ± 3.48	0.55
MCH pg	15.93 ± 0.80	16.19 ± 0.45	0.44
MCHC g/L	264.25 ± 11.61	261.75 ± 7.42	0.62
ALT U/L	40.61 ± 15.20	34.45 ± 11.02	0.37
AST U/L	141.75 ± 31.99	125.74 ± 21.02	0.26
TP g/L	56.05 ± 5.64	54.46 ± 5.61	0.58
ALB g/L	34.36 ± 3.17	33.63 ± 3.53	0.67
GLOB g/L	23.88 ± 3.17	23.33 ± 2.79	0.71
ALB/GLOB	1.45 ± 0.14	1.45 ± 0.11	0.97
BUN mmol/L	7.79 ± 1.08	7.50 ± 0.61	0.52
CREA umol/L	13.75 ± 4.39	13.06 ± 2.87	0.72

All numbers provided as mean ± standard deviation. ALB, albumin; ALT, alanine transaminase; AST, aspartate transaminase; BUN, blood urea nitrogen; CREA, creatinine; GLOB, globulin; HCT, hematocrit; HGB, hemoglobin; MCH, mean corpuscular hemoglobin; MCHC, mean corpuscular hemoglobin concentration; MCV, mean corpuscular volume; PLT, platelet; RBC, red blood count; TP, total protein; WBC, white blood count.

this study. Eight of the 16 ICR mice were included in the experimental group and eight in the control group. After

the presence of the nanocomposite-loaded with siRNA was verified in the lung, the experimental group showed no significant difference compared to the control group in body weight, organ coefficient, blood routine, blood biochemical index, or histopathological findings, suggesting that no acute toxicity occurred as a result of the nanocomposite-loaded siRNA (Table 1, Fig 2a–c).

Evaluation of efficacy of intratumor injection of PEG-PEI-EGFR-siRNA nanocomposites against residual lung tumor after microwave ablation (MWA)

There was no significant difference in the body weight growth curve between the four groups after tumor implantation ($P = 0.1798$) (Fig 3a). One mouse in the MWA + EGFR-siRNA group was excluded because the maximum transverse diameter did not meet the requirement. All MWAs were performed under the guidance of real-time ultrasound (Fig 3b). One mouse in the EGFR-siRNA group died during the anesthesia and one mouse in the MWA + NC-siRNA group died during the MWA procedure. To ensure the number of each group was matched for statistical purposes, one mouse in the NC-siRNA group was randomly removed for a total of five mice in each group. There was no significant difference in the calculated tumor volume after transfection or MWA between all groups on
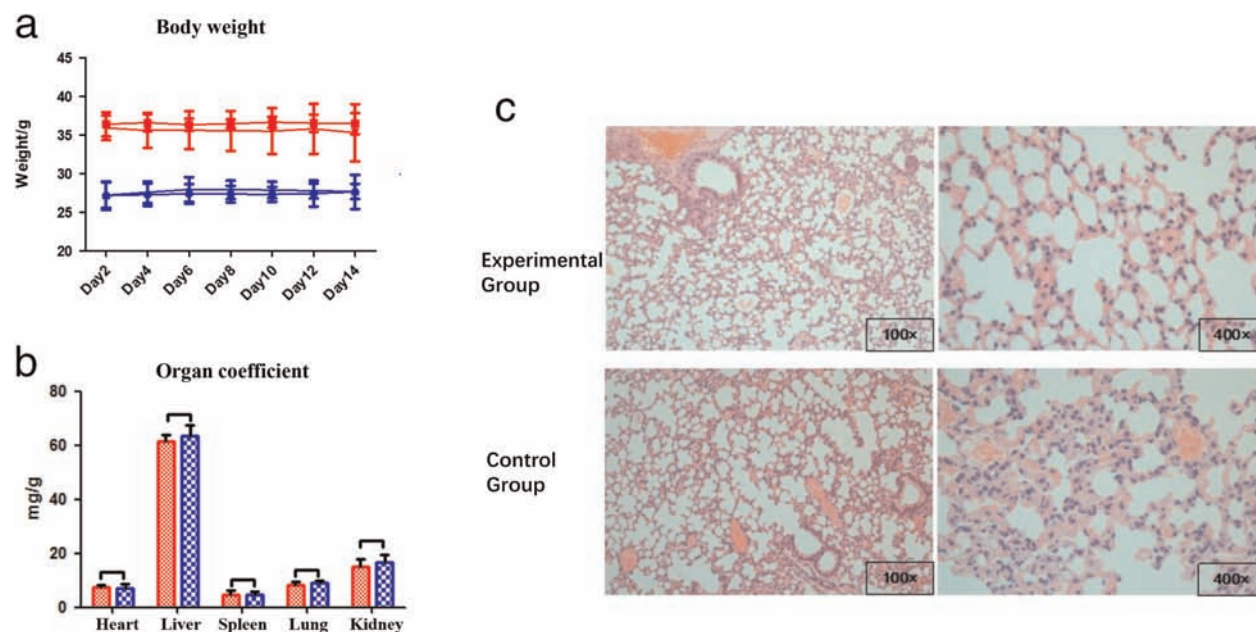

Figure 2 (**a**) Body weight changes in experimental and control mice. There was no significant difference in body weight between the experimental and control groups (*P* > 0.05). (—●—) Female mice in experimental group, (—■—) male mice in experimental group, (—▲—) female mice in control group, and (—▼—) male mice in control group. (**b**) Coefficients of visceral organs were compared and there was no significant difference between the groups (*P* > 0.05). (▨) Experimental group and (▨) control group. (**c**) Hematoxylin-eosin-stained lung tissue sections in the experimental and control groups showed no obvious inflammatory cell infiltration or alveolar structure changes, and no significant difference.
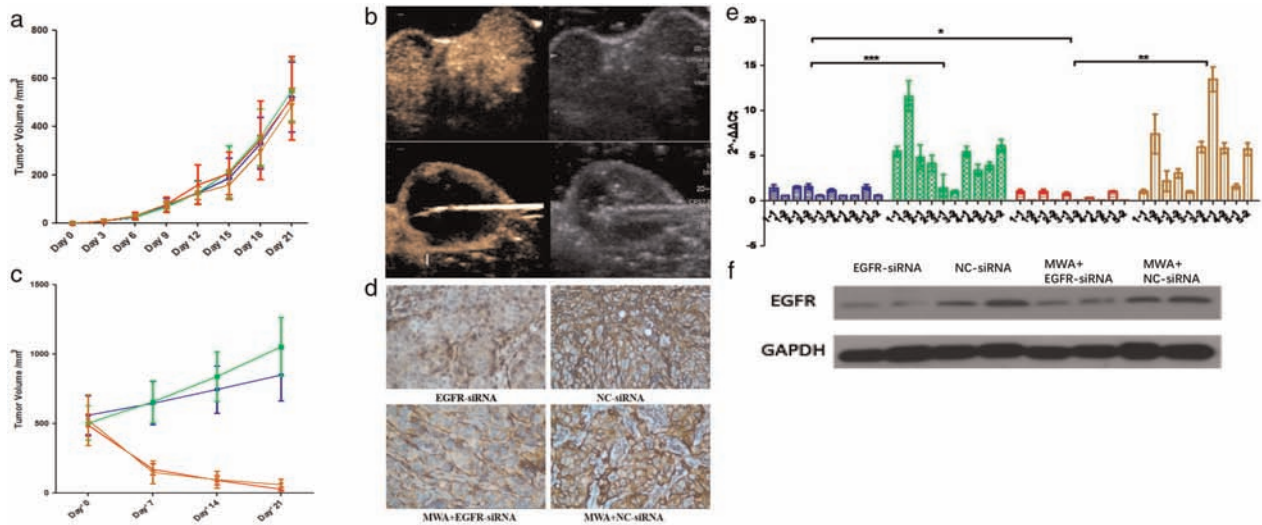
Figure 3 (**a**) There was no significant difference in tumor volume variation curve between the four groups (*P* > 0.05). (—●—) EGFR-siRNA, (—■—) NC-siRNA, (—▲—) MWA+EGFR-siRNA, and (—▼—) MWA+NC-siRNA. (**b**) Contrast ultrasound taken immediately after microwave ablation (MWA) showed that most tumors were necrotic and residual tumors existed in the peripheral region. (**c**) There was a significant decrease in tumor volume after treatment with MWA. At the endpoint, there was a statistically significant difference in tumor volume between the EGFR small interfering RNA (siRNA) and normal control (NC) siRNA groups (*P* = 0.037), and between the MWA + EGFR-siRNA and MWA + NC-siRNA groups (*P* = 0.033). (—●—) EGFR-siRNA, (—■—) NC-siRNA, (—▲—) MWA+EGFR-siRNA, and (—▼—) MWA+NC-siRNA. (**d**) Immunohistochemically stained tumor tissue showed low EGFR expression in the EGFR-siRNA group. (**e**, **f**). EGFR expression was lower in the EGFR-siRNA than in the NC-siRNA group, and lower in the MWA + EGFR-siRNA than in the MWA + NC-siRNA group, but higher in the MWA + EGFR-siRNA than in the EGFR-siRNA group. (▨) EGFR-siRNA, (▨) NC-siRNA, (■) MWA+EGFR-siRNA, and (▥) MWA+NC-siRNA.

days 0, 7, and 14 (*P* > 0.05). The endpoint was observed on the 21st day after treatment. The tumor volume was smaller in the EGFR-siRNA than in the NC-siRNA group (*P* = 0.037); smaller in the MWA + EGFR-siRNA than in the MWA + NC-siRNA group (*P* = 0.033); and smaller in the MWA + EGFR-siRNA than in the EGFR-siRNA group (*P* < 0.001) (Table 2, Fig 3c). The tumor weight was smaller in the EGFR-siRNA than in the NC-siRNA group (*P* = 0.037); smaller in the MWA + EGFR-siRNA than in the MWA + NC-siRNA group (*P* = 0.032); and smaller in the MWA + EGFR-siRNA than in the EGFR-siRNA group (*P* < 0.001). The tumor tissues were then stained with immunohistochemical staining. The level of EGFR in the tumor tissues was lower in the EGFR-siRNA than in the NC-siRNA group (*P* < 0.001); lower in the MWA + EGFR-siRNA than in the MWA + NC-siRNA group (*P* < 0.001); and not significantly different in the siRNA and MWA + EGFR-siRNA groups (*P* = 0.918) (Fig 3d). The mRNA expression of EGFR was lower in the EGFR-siRNA than in

the NC-siRNA group (*P* = 0.0009); lower in the MWA + EGFR-siRNA than in the MWA + NC-siRNA group (*P* = 0.0027); and lower in the MWA + EGFR-siRNA than in the EGFR-siRNA group (*P* = 0.0148) (Table 3). There was no significant difference between EGFR mRNA expression in the NC-siRNA and the MWA + NC-siRNA groups (*P* = 0.9975) (Fig 3e). EGFR protein expression was evaluated by Western blotting. The protein expression of EGFR was lower in the EGFR-siRNA than in the NC-siRNA group (*P* < 0.001); lower in the MWA + EGFR-siRNA than in the MWA + NC-siRNA group (*P* < 0.001); and lower in the MWA + EGFR-siRNA than in the siRNA group (*P* = 0.040) (Fig 3f).

Discussion

PEG-PEI-EGFR-siRNA nanocomposites were transfected to HCC 827 lung cancer cells showing high expression of EGFR protein. EGFR protein expression was knocked

Table 2 Comparison of tumor volume at different measurement times after treatment in each group (mm^3)

Group	Day 0	Day 7	Day 14	Day 21
EGFR-siRNA	559.90 ± 139.65	648.60 ± 154.77	745.78 ± 170.68	851.82 ± 187.39
NC-siRNA	504.79 ± 123.19	658.68 ± 149.80	840.58 ± 178.91	1052.82 ± 210.50
MWA + EGFR-siRNA	490.81 ± 78.55	172.68 ± 40.07	93.32 ± 31.64	28.28 ± 14.08
MWA + NC-siRNA	526.57 ± 182.63	151.46 ± 82.32	96.42 ± 61.73	60.29 ± 39.25

All numbers provided as mean ± standard deviation. MWA, microwave ablation; NC, normal control; siRNA, small interfering RNA.

Table 3 Expression levels of EGFR messenger RNA in each group at treatment endpoints

No. of nude mice	EGFR-siRNA	NC-siRNA	MWA + EGFR-siRNA	MWA + NC-siRNA
1–1	1.42 ± 0.34	5.47 ± 0.57	1.01 ± 0.20	1.01 ± 0.20
1–2	0.55 ± 0.02	11.55 ± 1.70	0.01 ± 0.00	7.40 ± 2.19
2–1	1.53 ± 0.11	4.83 ± 1.36	1.05 ± 0.21	2.17 ± 1.16
2–2	1.54 ± 0.33	4.13 ± 0.87	0.01 ± 0.00	3.03 ± 0.48
3–1	0.57 ± 0.04	1.43 ± 1.45	0.80 ± 0.14	1.00 ± 0.12
3–2	1.15 ± 0.14	1.01 ± 0.15	0.02 ± 0.00	5.93 ± 0.60
4–1	0.55 ± 0.02	5.45 ± 0.59	0.30 ± 0.06	13.47 ± 1.36
4–2	0.56 ± 0.01	3.37 ± 0.65	0.01 ± 0.00	5.81 ± 0.59
5–1	1.51 ± 0.26	3.87 ± 0.42	1.03 ± 0.09	1.58 ± 0.24
5–2	0.6 ± 0.02	6.06 ± 0.70	0.03 ± 0.00	5.72 ± 0.65
Mean ± SD	1.00 ± 0.48	4.72 ± 2.94	0.43 ± 0.47	4.71 ± 3.81
P value		0.0009		0.0027

All numbers provided as mean ± standard deviation (SD). MWA, microwave ablation; NC, normal control; siRNA, small interfering RNA.

down in HCC827 cells by downregulation of *EGFR* gene expression. Consequently, cell proliferation, invasion, and migration decreased, whereas cell apoptosis increased. No acute toxicity occurred in the biosafety test using 16 healthy ICR mice. Localized injection of PEG-PEI-EGFR-siRNA nanocomposites significantly inhibited the growth of human lung xenografts in mice and the growth of residual tumors after MWA.

In previous studies, RNAi technology was used to specifically block various genes that play an important role in the development of lung cancer, including apoptosis-related genes, proto-oncogenes, cell cycle-related genes, and drug resistance genes. Ma *et al.* found that after silencing the *p53* gene by RNAi, Anip973 lung cancer cells would stagnate at the G1 or G2/M phase, showing significant inhibition of cell growth.[21] Jin *et al.* proposed that c-Myc is abnormally expressed in malignant tumors, such as lung cancer.[22] They transfected c-Myc siRNA to lung cancer cells to inhibit the expression of c-Myc in lung cancer cells, and found that the transition from the G1 to S phase in the lung cancer cells was inhibited, thus terminating the proliferation of lung cancer cells. Zhang *et al.* transfected short hairpin RNA to A549 lung cancer cells to silence EGFR expression, and then detected the sensitivity of cancer cells to cisplatin.[23] In the experimental group, EGFR expression was inhibited by 85%, cell proliferation was inhibited by 63.3%, and sensitivity to cisplatin treatment was enhanced four-fold. In the same study, the tumor volume and weight of the animals was reduced by 75.06% and 73.08%, respectively. Thus, RNAi significantly inhibits EGFR expression and cell proliferation, as well as inducing cell cycle arrest and increasing the sensitivity of A549 lung cancer cells to cisplatin.

SiRNA suppresses target genes via inherent RNAi, which offers a potential treatment strategy to treat human cancers. However, the safe and efficient introduction of siRNA

into tumor tissues remains a hotspot and a challenging issue for scientists.[24] Although a viral vector can effectively transfect siRNA into a cell, it poses a great safety risk. At present, cationic polymers are widely recognized as gene carriers, and studies on cationic polymers are becoming increasingly advanced. Among these cationic polymers, PEI is an effective gene carrier with strong binding ability and a special molecular structure. Generally, PEI has a branched structure, and the third amino nitrogen atom present in each branched structure is prone to protonation; thus, PEI has a certain buffering capacity in different pH environments, which is also known as the proton sponge effect.[25] PEI also has the ability to dissolve lysosomal membranes. Therefore, the polymer of siRNA and PEI can avoid the degradation caused by an acidic environment in vivo. Furthermore, the high density of the positive charge of PEI can protect siRNA from being degraded by nucleases. In this study, we synthesized and optimized PEI, and grafted biocompatible PEG onto PEI to improve the stability and reduce the cationic toxicity of the polymer.

The high thermal and cavitation effects of MWA could increase membrane lipid fluidity, thereby increasing the fluidity of the antigen embedded in the lipid bilayer of the cell membrane, promoting antigen aggregation on the liquid surface of the cell membrane, and promoting antigen exposure, which is more conducive for the antibodies to bind to the antigens. The mechanical destruction of the cell membrane and other structures by MWA exposes the cytoplasm and nucleus to tumor antigens, thereby changing the immunogenicity of tumor tissues and enhancing the body's immune response to tumor tissues. Sensitivity to gene therapy may occur when the immune response is activated. In addition, some studies have shown that MWA may cause changes in cells, including changes in cell morphology, decreases in cell membrane permeability, decreases in cell division ability, inhibition of DNA synthesis, and

chromosome breakage. Studies have reported that MWA is directly involved in cell apoptosis, and that Bcl-2 and p53 may be involved in the apoptotic process.[26] These are possible mechanisms that may promote the effect of an intratumoral injection of EGFR-siRNA. However, these mechanisms require further study.

There were some limitations to this study. Firstly, the uniform stability of intratumoral injection of nanocomposites needs to be further improved, and the intratumoral injection method requires further optimization. Secondly, the interaction between MWA and the intratumoral injection was not discussed. In the future, an experimental group of MWA after intratumoral injection should be supplemented. Finally, whether MWA promotes the effect of SiRNA was not evaluated in this study.

In conclusion, an intratumoral injection of PEG-PEI-EGFR-siRNA nanocomposites significantly reduces EGFR expression and inhibits tumor growth. A localized intratumoral injection of PEG-PEI-EGFR-siRNA nanocomposites after MWA also significantly reduces EGFR expression and inhibits residual tumors.

Acknowledgments

Disclosure

No authors report any conflict of interest.

References

1 Ferlay J, Soerjomataram I, Dikshit R *et al.* Cancer incidence and mortality worldwide: Sources, methods and major patterns in GLOBOCAN 2012. *Int J Cancer* 2015; **136** (5): E359–86.

2 Hirsch FR, Scagliotti GV, Mulshine JL *et al.* Lung cancer: Current therapies and new targeted treatments. *Lancet* 2017; **389** (10066): 299–311.

3 Dupuy DE. Treatment of medically inoperable non-small-cell lung cancer with stereotactic body radiation therapy versus image-guided tumor ablation: Can interventional radiology compete? *J Vasc Interv Radiol* 2013; **24** (8): 1139–45.

4 Li G, Xue M, Chen W, Yi S. Efficacy and safety of radiofrequency ablation for lung cancers: A systematic review and meta-analysis. *Eur J Radiol* 2018; **100**: 92–8.

5 Ye X, Fan W, Wang H *et al.* Expert consensus workshop report: Guidelines for thermal ablation of primary and metastatic lung tumors (2018 edition). *J Cancer Res Ther* 2018; **14** (4): 730–44.

6 Li X, Qi H, Qing G *et al.* Microwave ablation with continued EGFR tyrosine kinase inhibitor therapy prolongs disease control in non-small-cell lung cancers with acquired resistance to EGFR tyrosine kinase inhibitors. *Thorac Cancer* 2018; **9** (8): 1012–7.

7 Dupuy DE, Fernando HC, Hillman S *et al.* Radiofrequency ablation of stage IA non-small cell lung cancer in medically inoperable patients: Results from the American College of Surgeons Oncology Group Z4033 (Alliance) trial. *Cancer Am Cancer Soc* 2015; **121** (19): 3491–8.

8 Timmerman R, Paulus R, Galvin J *et al.* Stereotactic body radiation therapy for inoperable early stage lung cancer. *JAMA* 2010; **303** (11): 1070–6.

9 Fernando HC, Landreneau RJ, Mandrekar SJ *et al.* Impact of brachytherapy on local recurrence rates after sublobar resection: Results from ACOSOG Z4032 (Alliance), a phase III randomized trial for high-risk operable non-small-cell lung cancer. *J Clin Oncol* 2014; **32** (23): 2456–62.

10 Ciardiello F, Tortora G. A novel approach in the treatment of cancer: Targeting the epidermal growth factor receptor. *Clin Cancer Res* 2001; **7** (10): 2958–70.

11 Tan DS, Yom SS, Tsao MS *et al.* The International Association for the Study of Lung Cancer consensus statement on optimizing management of EGFR mutation-positive non-small cell lung cancer: Status in 2016. *J Thorac Oncol* 2016; **11** (7): 946–63.

12 Fire AZ. Gene silencing by double-stranded RNA (Nobel lecture). *Angew Chem Int Ed Engl* 2007; **46** (37): 6966–84.

13 Yang J. Patisiran for the treatment of hereditary transthyretin-mediated amyloidosis. *Expert Rev Clin Pharmacol* 2019; **12** (2): 95–9.

14 Wood H. FDA approves patisiran to treat hereditary transthyretin amyloidosis. *Nat Rev Neurol* 2018; **14** (10): 570.

15 Solomon SD, Adams D, Kristen A *et al.* Effects of Patisiran, an RNA interference therapeutic, on cardiac parameters in patients with hereditary transthyretin-mediated amyloidosis. *Circulation* 2019; **139** (4): 431–43.

16 Das M, Musetti S, Huang L. RNA interference-based cancer drugs: The roadblocks, and the "delivery" of the promise. *Nucleic Acid Ther* 2019; **29**: 61–6.

17 Kim Y, Park T, Singh B *et al.* Nanoparticle-mediated delivery of siRNA for effective lung cancer therapy. *Nanomedicine* 2015; **10** (7): 1165–88.

18 Solazzo SA, Ahmed M, Schor-Bardach R *et al.* Liposomal doxorubicin increases radiofrequency ablation-induced tumor destruction by increasing cellular oxidative and nitrative stress and accelerating apoptotic pathways. *Radiology* 2010; **255** (1): 62–74.

19 Yang W, Ahmed M, Tasawwar B *et al.* Radiofrequency ablation combined with liposomal quercetin to increase tumour destruction by modulation of heat shock protein

production in a small animal model. *Int J Hyperthermia* 2011; **27** (6): 527–38.

20 Ahmed M, Kumar G, Navarro G *et al.* Systemic siRNA nanoparticle-based drugs combined with radiofrequency ablation for cancer therapy. *PLOS One* 2015; **10** (7): e128910.

21 Ma LL, Sun WJ, Wang Z, Zh GY, Li P, Fu SB. Effects of silencing of mutant p53 gene in human lung adenocarcinoma cell line Anip973. *J Exp Clin Cancer Res* 2006; **25** (4): 585–92.

22 Jin Z, Gao F, Flagg T, Deng X. Tobacco-specific nitrosamine 4-(methylnitrosamino)-1-(3-pyridyl)-1-butanone promotes functional cooperation of Bcl2 and c-Myc through phosphorylation in regulating cell survival and proliferation. *J Biol Chem* 2004; **279** (38): 40209–19.

23 Zhang M, Zhang X, Bai CX *et al.* Silencing the epidermal growth factor receptor gene with RNAi may be developed as a potential therapy for non small cell lung cancer. *Genet Vaccines Ther* 2005; **3**: 5.

24 Lee SH, Chung BH, Park TG, Nam YS, Mok H. Small-interfering RNA (siRNA)-based functional micro- and nanostructures for efficient and selective gene silencing. *Acc Chem Res* 2012; **45** (7): 1014–25.

25 Werth S, Urban-Klein B, Dai L *et al.* A low molecular weight fraction of polyethylenimine (PEI) displays increased transfection efficiency of DNA and siRNA in fresh or lyophilized complexes. *J Control Release* 2006; **112** (2): 257–70.

26 Song XL, Wang CH, Hu HY, Yu C, Bai C. Microwave induces apoptosis in A549 human lung carcinoma cell line. *Chin Med J (Engl)* 2011; **124** (8): 1193–8.